Pergamon

Int. J. Solids Structures Vol. 34, No. 5, pp. 569–580, 1997

0020-7683/96 $15.00 + .00

PII: S0020-7683(96)00039-X

EFFECT OF T-STRESSES ON THE PATH OF A THREE-DIMENSIONAL CRACK PROPAGATING QUASISTATICALLY UNDER TYPE I LOADING

A. A. AL-FALOU, H. LARRALDE and R. C. BALL
Cavendish Laboratory, Madingley Road, Cambridge CB3 0HE, U.K.

(*Received* 31 *October* 1995; *in revised form* 18 *April* 1996)

Abstract We consider a three-dimensional semi-infinite almost planar crack, propagating quasistatically under type I singular loading. Treating the distortion from planar geometry as a perturbation we evaluate the type II stress intensity factor arising from this distortion including the effect of non-singular T-stresses. Using these results we perform a linear stability analysis by assuming that the crack propagates locally in the direction of pure type I. We obtain a stability diagram as function of T_x and T_z reflecting the interaction between the effects due to the T-stresses and the stabilizing effect which arises from the perturbed geometry of the crack. From this we infer four types of stability of the crack: monotonous stability, oscillatory stability, monotonous instability and oscillatory instability. Additionally we find that for certain values of the ratio T_z/T_x a small interval of wavelengths of the perturbation will be selected as the crack propagates, so that the components corresponding to these wave lengths will grow expontially while all other components are suppressed. Copyright © 1996 Elsevier Science Ltd.

1. INTRODUCTION

The prediction of the path of a moving planar crack which is distorted by material imperfections is of high relevance not only in material science but also to throw light on the different regimes of roughness which are experimentally observed after the initiation of a crack. The general problem is not amenable to tractable analysis, and we will follow others in considering the case where the crack is only slightly distorted from planar geometry. We will also work within the simplification of linear, isotropic and homogeneous elasticity, and the regime of quasi-static crack propagation. The latter enables us to work with the equations of static linear elasticity. In the more general case of finite velocity of the crack tip we would have to perform a more complicated calculation using the dynamic equations of linear elasticity.

For a slightly curved purely two-dimensional crack, the path has already been calculated by Goldstein and Salganik (1974) as well as by Cotterell and Rice (1980). In the two-dimensional case the crack path depends significantly on the sign of the so called T-stress, the normal stress T_x acting in the direction of crack propagation. Expanding the stress field around the crack tip into

$$\sigma(\bar{r}) = \frac{K}{\sqrt{2\pi r}}\bar{\Sigma}(\Theta) + T + O(\sqrt{r})$$

T denotes the constant stress terms. The two dimensional results state that the crack becomes unstable if $T_x > 0$ and stable otherwise. In this context, the crack is defined to be stable if the crack edge remains below the initial tangential direction.

In this paper we present a calculation of the crack path for a three-dimensional crack after being distorted by an imperfection. In contrast to the two-dimensional result we get two interacting contributions to stability. As before, one part arises from the T-stress but there is an additional contribution to stability from the perturbed geometry of the crack. This additional term has recently been evaluated by Ball and Larralde (1995) and it has been verified experimentally (Larralde and Ball, 1995). Unlike the two dimensional case where only T_x occurs, we shall consider additional T-stress components contributing to

stability, i.e., T_{x}, T_{xz} and T_{z}. In what follows, we calculate the T-stress part of K_{II} and add the contribution of the perturbed geometry.

We assume that after the crack line is distorted by imperfections in the material, the crack propagates locally in the direction of pure type I, i.e., under the condition $K_{II} = 0$. This condition results from the requirement of propagation in the local direction of maximal hoop stress or maximal strain energy release rate (Lawn, 1993). Experiments show that even under the $K_{II} = 0$ condition a crack can split up into an array of small cracks if the angle φ of rotation of the principal stresses (through the presence of a non-zero K_{III}) exceeds a critical value φ_c (Somer, 1969; Hull, 1994). In this case a crack can propagate smoothly only as long as φ remains below the critical angle. However, the additional constraint $\varphi < \varphi_c$ is always obeyed within first order perturbation analysis. Writing the angle between the local tensile stress and the principal stress as $\varphi(K_{III}, K_I, K_I)$ and expanding to first order (it should be noted that K_{III}/K_I is a first order term and $\varphi(0, K_I) = 0$), we obtain that φ itself is of first order. Since a first order perturbation analysis requires that first order terms are small compared to all finite constants (φ_c in this case), it can be concluded that $\varphi < \varphi_c$ is always fulfilled in our analysis.

From the single remaining condition for smooth crack propagation, i.e., $K_{II} = 0$, we obtain an evolution equation for the crack edge. We will find the stability to depend on the zeros of the Laplace transformed kernel of the evolution equation. From this we derive a stability diagram as a function of T_x and T_z with surprising new features of stability for the three-dimensional crack. By instability, in this work, we mean that the distortion of the crack edge increases exponentially with respect to the unperturbed flat crack as the crack propagates whereas we refer to stability if the perturbed crack edge decays exponentially.

In order to keep our analysis tractable we have to impose certain restrictions on our assumptions. We consider a three-dimensional semi-infinite crack in an infinite isotropic material. The crack is assumed to move slowly compared with the speed of sound, which is a rather severe restriction, but permits analyzing the problem through the equations of static elasticity. Additionally in the quasi-static case the zero order displacements are those of a static planar crack. This also simplifies the calculation of higher order corrections to the stress field in contrast to dealing with the velocity dependent zero order terms of the fast moving crack (Ball and Larralde, 1995). Nevertheless, the more general case of a distorted crack which propagates with finite velocity turns out to be an analytically solvable task (Larralde and Ball, submitted for publication). But we emphasize the fact that this calculation which involves an application of the Wiener-Hopf technique is considerably more complicated than the derivation of the results presented here.

The deviation of the crack surface from planar geometry is treated as a small perturbation, where second and higher order terms are neglected. Our calculation includes only the out-of-plane perturbation; the in-plane perturbation of the crack edge is to first order a separable stability problem. It is assumed that the unperturbed planar reference crack is under type I loading characterized by a stress intensity factor k_I.

2. EQUATION DESCRIBING THE EVOLUTION OF THE CRACK TIP

As mentioned above, the total mode II stress intensity factor for the distorted crack, to first order, is given by superposition of the T-stress contribution and the contribution which arises from the distorted geometry. The latter, which we refer to as K_{II}^{φ}, has been calculated by Ball and Larralde (1995) where the authors evaluated the stress intensity factors in a frame of reference parallel to the unperturbed crack. Here, we present the transformation of K_{II}^{φ} into the frame of local forward direction. In the frame parallel to the unperturbed crack and with origin at the crack tip (see Fig. 1) the stress tensor reads as

$$\sigma(s') = \frac{k_I}{\sqrt{2\pi s}} \bar{\bar{\Sigma}}_I(\Theta') + \frac{K_{II}^{\varphi}}{\sqrt{2\pi s}} \bar{\bar{\Sigma}}_{II}(\Theta').$$

(s, Θ') and (s, Θ) are the polar coordinates of (s_1', s_2') and (s_1, s_2), respectively. Transforming into the frame of local forward direction and expanding in

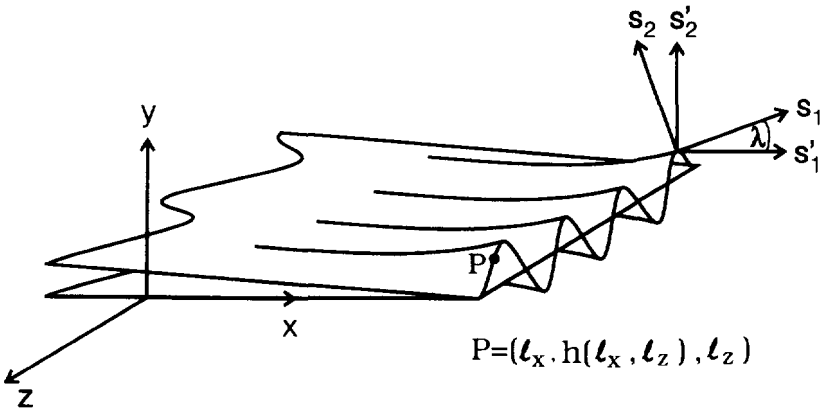

Fig. 1. Transformation of stress intensity factors in the frame of local forward direction.

$$\lambda = \left.\frac{\partial h(x,z)}{\partial x}\right|_{(x,z)=(\ell_x,\ell_z)}$$

we obtain (see Fig. 1)

$$\sigma(\bar{s}) = \frac{k_I}{\sqrt{2\pi s}}\bar{\bar{\Sigma}}_I(\Theta) + \frac{k_I}{\sqrt{2\pi s}}\frac{\partial h(\ell_x,\ell_z)}{\partial \ell_x}\frac{\partial \bar{\bar{\Sigma}}_I(\Theta)}{\partial \Theta} + \frac{K_{II}'}{\sqrt{2\pi s}}\bar{\bar{\Sigma}}_{II}(\Theta) \tag{1}$$

where higher order terms are neglected and where $(\ell_x, h(\ell_x,\ell_z),\ell_z)$ are the coordinates of the crack edge. Observing that

$$\frac{\partial \bar{\bar{\Sigma}}_I(\Theta)}{\partial \Theta} = 2\bar{\bar{\Sigma}}_{II}(\Theta) \qquad \text{and} \qquad K_{II}' = \tfrac{1}{2}(1-2\alpha)|k|h_k(\ell_x)k_I$$

(as stated by Ball and Larralde, 1995) we obtain

$$K_{II}^{a}(\ell_x,\ell_z) = \left(\frac{1}{2}\frac{\partial h_k(\ell_x)}{\partial \ell_x}k_I + \frac{1}{2}(1-2\alpha)|k|h_k(\ell_x)k_I\right)e^{ik\ell} \tag{2}$$

where the constant α is given in terms of Poisson's ratio ν by $\alpha = \nu/(2-\nu)$. Here, $h_k(x)$ is the Fourier transform of the crack surface parametrisation $h(x,z)$. Linearity of the equations of elasticity enables us to write K_{II} as superposition of its Fourier components with respect to the z variable. Hence, without loss of generality, we may perform the following calculation for a single term of the Fourier spectrum (with respect to the z-variable) of K_{II} and the perturbation of the crack surface $h(x,z)$.

To eqn (2) we add the contribution of the T-stress to K_{II}, which will be calculated below. We need to keep only T_x, T_{xz} and T_z since all other components of T are zero. We calculate the T-stress contribution to K_{II} by applying the weight function method to a planar crack with straight crack edge. The weight function returns the singular stress field around the crack edge as a reaction to a pair of opposite point forces, each applied on one face of the planar crack. Thus, the complete singular stress field for a planar crack can be obtained by superposition of all tractions on the crack surface.

The T-tractions on the perturbed crack surface are obtained from

$$\bar{f}(x,z) = T\cdot\bar{n}(x,z) = -\left(\frac{\partial h(x,z)}{\partial x}T_x + \frac{\partial h(x,z)}{\partial z}T_{xz}, 0, \frac{\partial h(x,z)}{\partial x}T_{xz} + \frac{\partial h(x,z)}{\partial z}T_z\right) \tag{3}$$

If $\bar{n}(x,z)$ is the normal vector to the crack surface. Since these tractions are already of first order, it is equivalent to evaluate them on distorted crack surface or to evaluate them on a

planar crack to first order perturbation analysis. Another way to obtain this result is to consider a one-to-one mapping which maps the whole three-dimensional space onto itself and in particular the perturbed crack surface onto a plane. It is a crucial characteristic of first order perturbation analysis that such a mapping exists and that it has the form $I+\varepsilon$ (I is the identity operator and ε a first order mapping). Parametrising the distorted crack by this mapping, inserting for the variables into the tractions in (3) and expanding the expression results in the same tractions but for a flat crack.

From this it follows that we can apply the three-dimensional weight function for a flat crack from Sih (1973). Each Fourier component of the weight function for mode II reads as

$$W_{\mathrm{II}}(x', z', z) = \frac{1}{\pi} \frac{\mathrm{e}^{kx}}{\sqrt{2\pi(-x')}} (Q(1+2\alpha|k|x'|) + Ri\alpha k(-x'))\mathrm{e}^{ik(z-z')} \tag{4}$$

where a balanced point force $(Q, 0, R)$ is applied at the point (x', z') on each face of the flat crack with straight crack edge on the z-axis. Finally, the Fourier transformed T-tractions from (3) have to be inserted into this expression. After evaluating the integral over x', z' we obtain

$$\begin{aligned} K_{\mathrm{II}}^{T}(l_x, l_z) = \mathrm{e}^{ikl_z}\left(-\sqrt{\frac{2}{\pi}}\right)\int_0^{l_x} \mathrm{d}x' \frac{\mathrm{e}^{k(l_x-x')}}{\sqrt{l_x-x'}}\Bigg[T_x \frac{\partial h_k(x')}{\partial x'}(1+2\alpha|k|(l_x-x')) \\ - T_z 2\alpha h_k(x')k^2(l_x-x') \\ + iT_{xz}\left(h_k(x')k(1+2\alpha|k|(l_x-x')) + 2\alpha k(l_x-x')\frac{\partial h_k(x')}{\partial x'}\right)\Bigg] \end{aligned} \tag{5}$$

as the result for the contribution of the T-stresses to K_{II}. Note that the derivation of this result is of different nature from calculating the contribution to K_{II} which arises from the perturbed geometry of the crack: the reason for this is that the latter case involved a singular term around the crack edge whereas the T-stress calculation contains only regular terms. In other words for the T-stress contribution it is equivalent to consider the crack edge to be at the position of the perturbed crack or to coincide with the tip of the unperturbed planar crack, very much in contrast to the calculation of the contribution from the perturbed geometry where the position of the crack edge played a central role in evaluating the stress intensity factors.

The propagation of the crack is determined by the condition that $K_{\mathrm{II}} = 0$. Adding both contributions for K_{II} from eqns (2) and (5) and setting the total mode II stress intensity factor to zero we finally obtain the integral equation which determines the direction of crack propagation

$$\begin{aligned} &\frac{\partial h_k(l_x)}{\partial l_x} + (1-2\alpha)|k|h_k(l_x) - \frac{2}{k_{\mathrm{I}}}\sqrt{\frac{2}{\pi}}\int_0^{l_x} \mathrm{d}x' \frac{\mathrm{e}^{k(l_x-x')}}{\sqrt{l_x-x'}}\Bigg[T_x \frac{\partial h_k(x')}{\partial x'}(1+2\alpha|k|(l_x-x')) \\ &- T_z 2\alpha h_k(x')k^2(l_x-x') + iT_{xz}\left(h_k(x')k(1+2\alpha|k|(l_x-x')) + 2\alpha k(l_x-x')\frac{\partial h_k(x')}{\partial x'}\right)\Bigg] \\ &\qquad = f_k(l_x) + g_k(l_x) =: F_k(l_x). \end{aligned} \tag{6}$$

The driving terms on the RHS are of two origins. First $f_k(l_x)$ arises from separating the convolution integral (5) into a part from 0 to l_x and a part from $-\infty$ to 0. The integral from $-\infty$ to 0 is defined as $f_k(l_x)$. We assume the crack surface $h(x, z)$ to be predetermined in the range $x < 0$, so that $f_k(l_x)$ is a known function which must be Laplace transformable. Secondly we add a noise term $g_k(x)$ due to the possible deviations of the material from our

assumptions as would result, for example, in the presence of inclusions and other defects. We will continue our calculation with $F_k(l_1)$ representing the general inhomogeneity on the right hand side of the equation.

This formulation includes the special case of a constant inhomogeneity term which is treated by Cotterell and Rice (1980). If we set $F_k(l_1) = -2k_{II}/k_I$ and we then take the limit $k \to 0$ in eqn (6), we obtain the two dimensional result of Cotterell and Rice (1980) (i.e., eqn (43)).

Applying the Laplace transform (this s is not to be confused with the s used in eqn (1))

$$\hat{h}(s) := \int_0^\infty \mathrm{d}x\, \mathrm{e}^{-sx} h(x) \tag{7}$$

to eqn (6) and rearranging terms gives (from here on the k-dependence will be left implicit) :

$$\hat{h}(s) - \frac{h(0)}{s} = -\frac{h(0)}{s} \frac{|k|(1-2\alpha)(s+|k|)^{3/2} + \frac{2\sqrt{2}T_x}{k_I}\alpha k^2 - i\frac{2\sqrt{2T_{xz}}}{k_I}k(s+|k|+\alpha|k|)}{K(s)} + \frac{\hat{F}(s)(s+|k|)^{3/2}}{K(s)} \tag{8}$$

where

$$K(s) := (s+|k|-2\alpha|k|)(s+|k|)^{3/2} - \frac{2\sqrt{2}T_x}{k_I}s(s+|k|+\alpha|k|) + \frac{2\sqrt{2}T_z}{k_I}\alpha k^2 - i\frac{2\sqrt{2T_{xz}}}{k_I}(1+\alpha)k(s+|k|). \tag{9}$$

We choose the branch cut of $K(s)$ to be on the negative real axis. Introducing dimensionless parameters and translating the variable such that the branch point is at the origin

$$z := 1 + \frac{s}{|k|} \qquad \beta_x := \frac{2\sqrt{2}T_x}{k_I\sqrt{|k|}} \qquad \beta_z := \frac{2\sqrt{2}T_z}{k_I\sqrt{|k|}} \qquad \beta_{xz} := \frac{2\sqrt{2}T_{xz}}{k_I\sqrt{|k|}}\,\mathrm{sign}(k) \tag{10}$$

z denotes a complex variable in what follows and should not be confused with the z-coordinate above. We than obtain for the Laplace inverse transform

$$h(l_1) - h(0) = \mathrm{e}^{-kl_1} \int_{\sigma-i\infty}^{\sigma+i\infty} \mathrm{d}z \mathrm{e}^{z-kl_1} \frac{q(z)}{p(z)(z-1)} \tag{11}$$

with

$$q(z) = -h(0)((1-2\alpha)z^{3/2} + \beta_z\alpha - i\beta_{xz}(z+\alpha)) + \hat{F}(|k|(z-1))z^{3/2}(z-1) \tag{12}$$

$$p(z) = z^{5/2} - \beta_x z^2 - 2\alpha z^{3/2} + ((1-\alpha)\beta_x - i(1+\alpha)\beta_{xz})z + \alpha(\beta_x + \beta_z). \tag{13}$$

The position of the zeros ζ_i of the function $p(z)$ in the complex plane determines the stability of the crack. In general the zeros are of order one and $\zeta_i \neq 1$ as well as differing from the poles of $\hat{F}(|k|(z-1))$. Under suitable conditions on the function $z \to \hat{F}(|k|(z-1))$, the Laplace inverse transform in (11) takes the form

$$h(l_x) = \sum_i \frac{q(\zeta_i)}{p'(\zeta_i)(\zeta_i - 1)} e^{(\zeta_i - 1)k l_x} + e^{-k l_x} \text{(branch cut integral)}$$
$$+ \sum_{\text{poles of } \hat{F}} \text{terms arising from poles of } \hat{F}. \tag{14}$$

For fixed k and $l_x \to \infty$ the height $h_k(l_x)$ of the crack edge is determined by the first term in eqn (14). If one of the zeros ζ_i of $p(z)$ has a real part greater than 1 then $h_k(l_x)$ would grow exponentially. We refer to this case as unstable crack propagation. If all zeros ζ_i have a real part smaller than or equal to 1 we say that the crack moves in a stable manner.

The function p from eqn (11) can be written as $p(z) = (\sqrt{z} - \xi_1) \ldots (\sqrt{z} - \xi_5)$. The actual zeros of $p(z)$ are ξ_i^2 with $\mathrm{Re}(\xi_i) \geqslant 0$, and we assume the ξ_i to be pairwise different and not equal to 1.

For our purposes it suffices to perform the inverse Laplace transform explicitly if $F_k(l_x)$ takes the special form $F_k(l_x) = \Theta_k + \Delta_k \delta(l_x)$. This includes the two most relevant cases. First the case which is treated by Cotterell and Rice, where $\Delta_k = 0$ and $\Theta_k = -2k_{II}/k_I$. Secondly the case where the crack edge is considered to be far away from the imperfection. In the vicinity of the imperfection the abrupt change of the direction of the crack coincides with a temporary jump of K_{II} to a non-zero value. We assume that far away from the imperfection this jump of K_{II} can be equivalently described by a sharp peak. This case is given by $\Delta_k = h_k(0^-) - h_k(0)$ and $\Theta_k = 0$. Evaluating the branch cut integral in eqn (14) and adding the other terms we obtain

$$h(l_x) = \sum_{i=1}^{5} \frac{1}{2} \frac{q_+(\xi_i^2)}{p'_+(\xi_i^2)(\xi_i^2 - 1)} e^{(\xi_i^2 - 1)k l_x} \operatorname{erfc}(-\xi_i \sqrt{|k| l_x})$$
$$+ \frac{\Theta}{|k|} \frac{(1-2\alpha) + (i\beta_{xz}(1+\alpha) - \beta_z \alpha) \operatorname{erf}(\sqrt{|k| l_x})}{(1-2\alpha)^2 + \beta_{xz}^2 (1+\alpha)^2 - \beta_z^2 \alpha^2 + 2i\beta_{xz}\beta_z \alpha(1+\alpha)} \tag{15}$$

where erf denotes the error function and erfc the complementary error function. The index $+$ indicates that square roots of the form $\sqrt{u^2}$ in that function shall always be evaluated as $+u$ (otherwise it would be $\sqrt{u^2} = -u$ if $\mathrm{Re}(u) \leqslant 0$). It should be noticed that $q_+(\xi_i^2)$ contains Δ_k and Θ_k.

In the second case, the constant term vanishes ($\Theta_k = 0$) and in what follows we shall refer to this situation. We then examine the zeros of the function $p(z)$ to separate regions of instability from regions of stability.

3. STABILITY ANALYSIS WITH RESPECT TO T-STRESS COMPONENTS

In what follows we restrict our consideration, for simplicity, to the case $\beta_{xz} = 0$. Including the β_{xz} contribution to stability is a straight forward exercise, but then we would finally get a three dimensional stability diagram which is much less illustrative than the two-dimensional diagram presented below (Fig. 4). With $\beta_{xz} = 0$, p takes the form

$$p(z) = z^{5/2} - \beta_x z^2 - 2\alpha z^{3/2} + (1-\alpha)\beta_x z + \alpha(\beta_x + \beta_z). \tag{16}$$

In this case we first determine the actual number of zeros of p. The number of zeros can be derived from Rouchés theorem (Saff and Snider, 1976). To apply the theorem we observe that (for $\alpha > 0$)

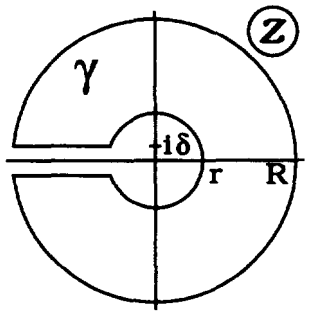

Fig. 2. The contour γ. The limits are to be taken as $R \to \infty$, $r \to 0$ and $\delta \to 0$.

$$|p(z) - (z^{5/2} + \varepsilon(\beta_1 + \beta_2))| < |p(z)| \tag{17}$$

on γ if $\varepsilon > 0$ is chosen small enough. The contour γ is shown in Fig. 2.

Then, Rouchés theorem states that $p(z)$ has the same number of zeros in $\mathbb{C} \setminus (-\infty, 0]$ as the function $z^{5/2} + \varepsilon(\beta_1 + \beta_2)$. From this it follows that $p(z)$ has three zeros for $\beta_1 + \beta_2 < 0$ whereas it has two zeros for $\beta_1 + \beta_2 > 0$.

All the zeros can be calculated numerically from eqn (16) as function of β_1 and β_2. We emphasize that the parametrisation of the crack edge $h(l_1)$ in eqn (14) is Fourier transformed in its z coordinate. In order to get the path of the crack edge in real space we have to collect over k all solutions $h_k(l_1)$ from eqn (14). On the other hand the dimensionless parameters, as for example

$$\beta_1 = \frac{2_1 \sqrt{2} T_1}{k_{1\sqrt{}} |k|},$$

depend on k as well. Varying k means to move on a radial line in the β_1, β_2 plane where the angle of such a radial line is given by $\tan\phi = T_2/T_1$. Translated into the β_1, β_2 plane collecting all solutions $h_k(l_1)$ over k means that for fixed T-stresses T_1, T_2 we have to evaluate the zeros of $p(z)$ on radial lines. It should be noted that the zeros z of $p(z)$ occur in the relevant exponential factor in eqn (14) through $s = (z-1)|k|$ (s is the transformation variable of the Laplace transform as defined in eqn (7)).

We present the zeros in Fig. 3 on radial lines in the β_1, β_2 plane for different angles. Between $\phi = -\frac{3}{8}\pi$ and $\phi = \frac{3}{8}\pi$ the main features of the shape of the zeros do not change. For our stability considerations we focus our attention on the zero with biggest real part since the exponential term associated with it will dominate the path of the crack edge $h_k(l_1)$ in eqn (14).

The asymptotic expansion of the dominant zero with biggest real part as $\beta \to \infty$ (i.e., $k \to 0$) are given by:

$$z \sim \beta_1^2 \qquad \text{for } -\frac{\pi}{2} < \phi < \frac{\pi}{2}$$

$$z \sim \alpha^{2/5} e^{i(2/5)\pi} \beta_2^{2/5} \qquad \text{for } \phi = \frac{\pi}{2}$$

$$z \sim \alpha^{2/5} \beta_2^{2/5} |k|^{4/5} - |k| \qquad \text{for } \phi = -\frac{\pi}{2}$$

$$z \sim z_1 + z_1^{3/2} \frac{z_1 - 2\alpha}{\sqrt{(1+\alpha)^2 + 4\alpha \tan\phi}} \frac{1}{\beta \cos\phi} \qquad \text{for } \frac{\pi}{2} < \phi < \frac{3}{2}\pi$$

with

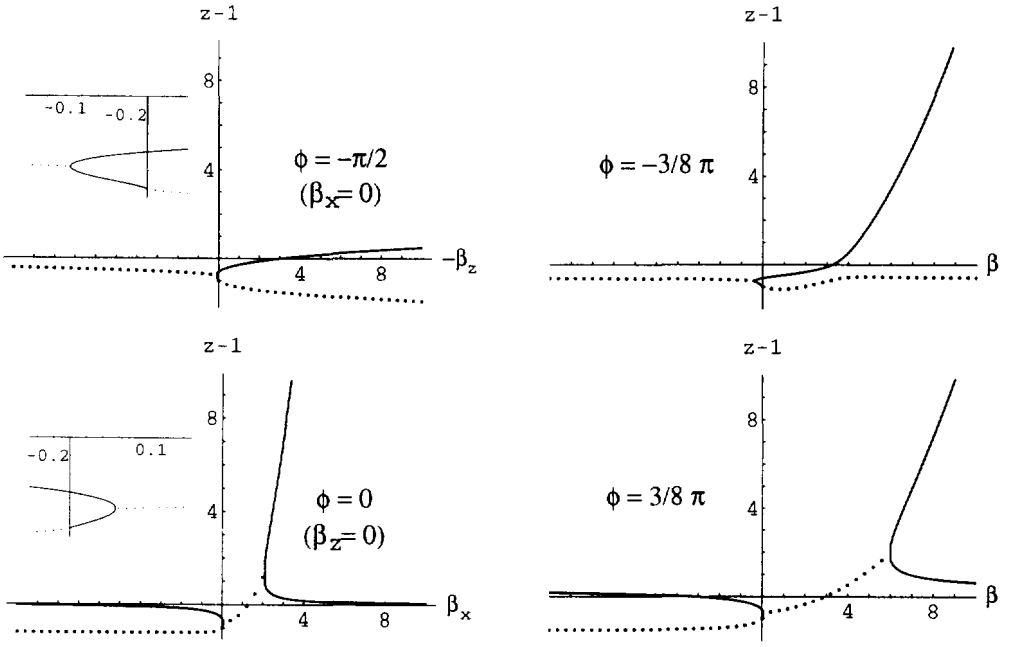

Fig. 3. The zeros of the function $p(z)$ on radial lines in the β_x, β_z plane. We set $\beta_x = \beta\cos\phi$ and $\beta_z = \beta\sin\phi$ in eqn (16). The negative β axis coincides with an angle of $\phi + \pi$. Connected lines denote a real zero; dotted lines denote the real part of a complex zero (and of its complex conjugate); insets show detail near the origin. We chose $\nu = 1/3$ for the Poisson ratio (i.e., $\alpha \equiv \nu/(2-\nu) = 0.2$).

$$z_1 = \frac{1-\alpha}{2} + \frac{1}{2}\sqrt{(1+\alpha)^2 + 4\alpha\tan\phi}.$$

We set $\beta_x = \beta\cos\phi$ and $\beta_z = \beta\sin\phi$ as the zero is evaluated along a radial line in β_x, β_z plane. In the two-dimensional limit $k \to 0$, only the expansion for $\phi = 0$ survives. In this case the asymptotic behaviour of $s = |k|(z-1)$ as the relevant exponential factor (see also eqns (14) and (10)) is given by

$$s \sim \left(\frac{2\sqrt{2T_x}}{k_1}\right)^2 - |k|.$$

This recovers the result of Cotterell and Rice (1980) in the two-dimensional limit.

But, for finite wave vector k, we notice several significant differences to the two-dimensional case. First, a region occurs where, for certain wave vectors, the perturbation may oscillate as it decreases or increases. To this case we refer as oscillatory stability or oscillatory instability respectively.

Secondly we consider the case of pure T_x ($\phi = 0$). For β_x small enough (i.e., small wavelength) we obtain stability although T_x is positive (see the inset). Moreover as β_x becomes more negative (i.e., larger wavelength of the perturbation) the zero grows and approaches one from below. This means that in the case $T_x \leqslant 0$ perturbations are less suppressed as their wavelength decreases. These effects results from the interaction of the T-stress with the stabilizing effect which arises from the perturbed geometry.

Although it is impossible to calculate the zeros explicitly (since $p(z)$ leads to a polynomial of 5th order after substituting $z \to u^2$), we may get explicit expressions for relevant special points. For example we are interested in the values of β_x and β_z at which the real part of the zero becomes 1 because these values separate regions of stability from regions of instability. This additional condition eliminates the 5th order term in $p(z)$. We obtain two polynomials of 4th order where the order of both polynomials can be reduced successively. We end up with an implicit equation for these special values of β_x, β_z.

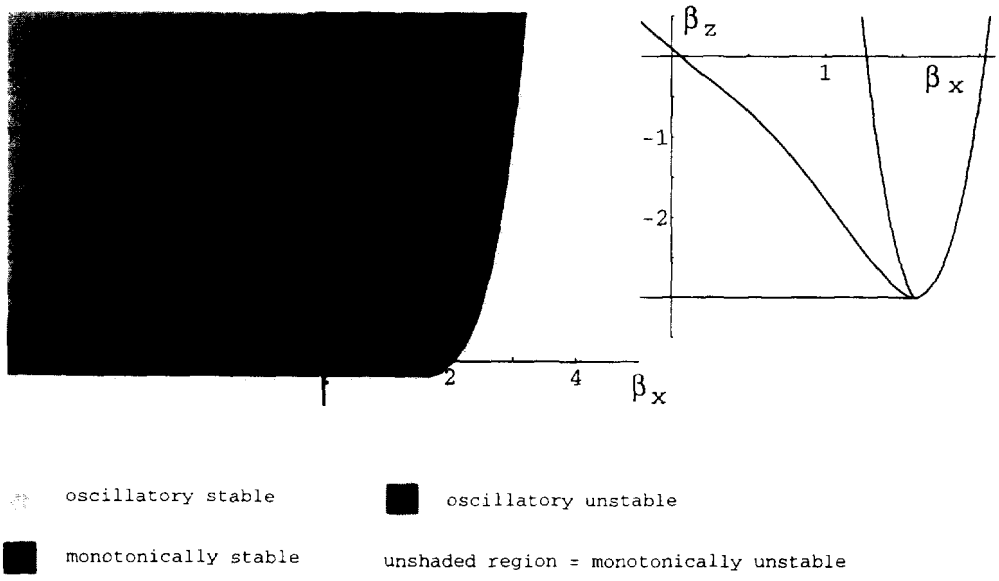

Fig. 4. Stability diagram as function of β_x and β_z. It should be noticed the different scaling of β_x and β_z. The Poisson ratio is $\nu = 1/3$ ($\alpha = 0.2$). The inset on the right hand side presents an enlarged region around the origin.

Similarly we calculated the points (β_x, β_z) that enclose the regions of oscillations, i.e., regions of dominating zeros with imaginary part. Thus we finally obtain a stability diagram which is presented in Fig. 4. The stability diagram provides a useful tool for experiments. As T_x and T_z are fixed, all Fourier components of the perturbed crack edge are given on a radial line with angle $\tan\phi = T_z/T_x$ in the β_x, β_z plane. Then the stability diagram shows the Fourier components that are suppressed exponentially (i.e., the section of the radial line which lies in a region of stability) and the components that increase exponentially (i.e., the section of the line that lies in a region of instability). Additionally it shows in each case whether the Fourier component is evolving in a monotonically or oscillatory manner.

It should be noticed that perturbations with sufficiently small wavelength are always suppressed since a sufficiently small vicinity of the origin is placed completely within regions of stability. We also calculated the asymptotic behaviour of all lines and the coordinates of their crossing point in Fig. 4 as to provide sufficient information to sketch a stability diagram for other values of the Poisson ratio.

The asymptotic expansions as $\beta_x \to \pm\infty$ are further elaborated in Appendix B:

$$\beta_z \sim -\frac{(1+\alpha)^2}{4\alpha}\beta_x$$

for the line which separates the monotonically from the oscillatory stable region,

$$\beta_z \sim \frac{256}{3125\alpha}\beta_x^5$$

for the line which separates the monotonically from the oscillatory unstable region,

$$\beta_z \sim \left(-\frac{4(1+\alpha)^4}{\alpha^3}\beta_x^2\right)^{1/3}$$

for the border line between the oscillatory stable region and the oscillatory unstable region,

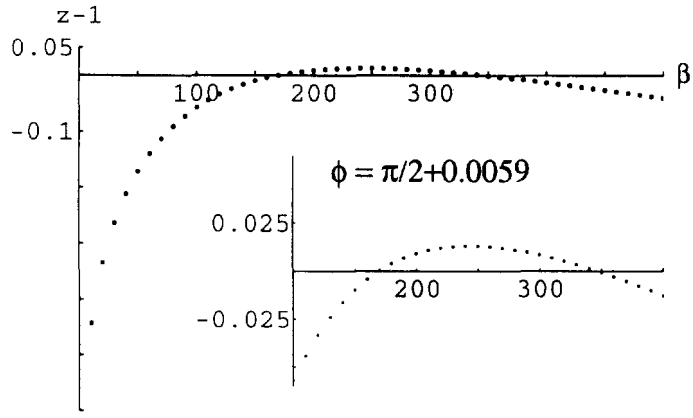

Fig. 5. Real part of the zeros of the function $p(z)$ along a radial line with angle $\phi = \pi/2 + 0.0059$ to illustrate the effect of selecting perturbations with special wavelengths ($\alpha = 0.2$).

$$(\beta_1, \beta_2) = \left(\frac{5-6\alpha}{2(1+\alpha)}, -\frac{1-2\alpha}{\alpha} \right)$$

for the crossing point of all curves.

From the stability diagram we can infer another significant result. For angles in the range of $\pi/2 < \phi \leqslant \pi/2 + 0.0061$ we observe that the radial line cuts the border line between the regions of oscillatory stability and oscillatory instability. But since this line grows faster than the linear radial line there has to be a second crossing point further up. As a result of this a closed interval of the radial line lies in the region of oscillatory instability whereas the rest of the radial line lies in the region of oscillatory stability. Hence Fourier components within a special range of wavelengths grow exponentially whereas all other Fourier components are suppressed. Thus the crack acts as a filter for perturbations with special wavelengths by adjusting T_1 and T_2. In order to illustrate this effect we present the zero along a radial line with angle in the range $\pi/2 < \phi \leqslant \phi_0$ in Fig. 5. The numerical value for the grazing angle is $\phi_0 = \pi/2 + 0.0061$ if $\alpha = 0.2$.

4. CONCLUSIONS

Adding the contribution of T-stress to a first order stability analysis of a slightly perturbed semi-infinite crack under type I loading yields a stability diagram as shown in Fig. 4. This diagram results from the interaction of T-stress components T_1, T_2 and stabilising effects which arise from the distorted geometry of the crack. The main features are regions of monotonic stability, oscillatory stability, monotonic instability and oscillatory instability. Additionally we observe that for certain ratios T_2/T_1 the crack acts as a filter for perturbations around a selected wavelength.

In the two-dimensional limit we recover former results.

Although we obtain the outcome of our calculation as an interaction of different effects, some of our results could have been anticipated by intuitive considerations. For example, as shown in the second inset of Fig. 3 (the case $\phi = 0$), for a fixed wave number k ($k \neq 0$) in the absence of T_2, the presence of a small positive T_1 renders the perturbation more stable than the situation with negative T_1. This is in contrast to the two dimensional case in which positive and negative T_1 stresses were destabilizing and stabilizing respectively (as mentioned previously, our results indeed bear this situation in the limit $k \to 0$). How our result comes about can be understood through the following argument. In the absence of T-stress, the perturbed geometry of the crack gives rise to K_{II}^{q} which deviates the crack back to the plane of reference of the unperturbed crack. The presence of a positive T_1 stress gives rise to a mode II stress intensity factor which couples with the x-derivative of the perturbation, and acts to increase the magnitude of this derivative. If this increase is small, then the net effect of the T-stress is to enhance the decay rate of the perturbation. Of course,

with hindsight, it is apparent that as the magnitude of the T-stress increases, it eventually bends the trajectory of the crack so much that it overshoots the reference plane and the decay becomes oscillatory first and eventually unstable. Similarly, the presence of negative T_x acts to diminish the magnitude of the x-derivative of the trajectory, effectively reducing the decay rate of the perturbation.

The variety of phenomena reflected in the stability diagram arises from the fact that introducing T-stresses gives rise to the length scales $(k_I/T_x)^2$ and $(k_I/T_z)^2$, against which the wavelength of the perturbation can be measured. In particular, a careful choice of parameters can give rise to the selection of an interval of wavelengths whose Fourier components grow expontially, while all other components are damped.

Finally we should mention that the effect of T_{xz} has not been explored, although eqn (13) provides the full polynomial for extending our formulation to include those.

Acknowledgements—A. A. Al-Falou gratefully acknowledges financial support from the German Acadamic Exchange Service DAAD ("DAAD-Doktorandenstipendienprogramm aus Mitteln des zweiten Hochschulsonderprogramms"). Dr H. Larralde is funded by EPSRC (formerly SERC).

REFERENCES

Ball, R. C. and Larralde, H. (1995). Linear stability analysis of planar straight cracks propagating quasistatically under type I loading. *Int. J. Fract.* **71**, 365–377.
Cotterell, B. and Rice, J. R. (1980). Slightly curved or kinked cracks. *Int. J. Fract.* **16**, 155–169.
Goldstein, R. V. and Salganik, R. L. (1974). Brittle fracture of solids with arbitrary cracks. *Int. J. Fract.* **10**, 507–523.
Hull, D. (1994). The effect of mixed mode I/III on crack evolution in brittle solids. *Int. J. Fract.* **70**, 59–79.
Larralde, H. and Ball, R. C. (1995). The shape of slowly growing cracks. *Europhys. Lett.* **30**, 87–92.
Larralde, H. and Ball, R. C. Dynamic stress intensity factors and stability of three dimensional planar cracks. Submitted for publication.
Lawn, B. (1993). *Fracture of Brittle Solids*. Cambridge University Press, Cambridge, U.K.
Saff, E. B. and Snider, A. D. (1976). *Fundamentals of Complex Analysis for Mathematics, Science, and Engineering*. Prentice-Hall.
Sih, G. C. (1973). *Handbook of Stress Intensity Factors*. Lehigh University, Bethlehem Pennsilvania.
Sommer, E. (1969). Formation of fracture lances in glass. *Engng Fract. Mech* **1**, 539–546.

APPENDIX A

Mathematical symbols and nomenclature

$\bar{\sigma}(\bar{r})$	stress tensor at the position $\bar{r}$
K	stress intensity factor (see also Lawn, 1993), for example K_I denotes the mode I stress intensity factor
k_I	mode I stress intensity factor of the unperturbed crack
$\bar{\Sigma}(\Theta)$	angular part of the singular stress (see also Lawn, 1993)
$\bar{\Sigma}_I$	angular part of the mode I singular stress tensor
T	T-stress tensor, i.e., the constant tensor in an expansion of the stress tensor around the crack tip
$O(\sqrt{r})$	order of $\sqrt{r}$
K_{II}^{p}	mode II stress intensity factor which arises from the perturbed geometry of the crack (Ball and Larralde, 1995)
K_{II}^{t}	mode II stress intensity factor which arises from the T-stress contribution
$(l_x, h(l_x, l_z), l_z)$	coordinates of points on the crack edge
W_{II}	mode II weight function (Sih, 1973)
$\hat{h}$	Laplace transform of the function h
erf(x), erfc(x)	errorfunction and complementary errorfunction, respectively
$\alpha = \nu/(2-\nu)$	where ν is Poisson's ratio
$\mathbb{C}$	complex plane.

APPENDIX B

Details of the calculation of stability lines

Mapping out the zeros of $p(z)$ for different values of β_x and β_z (see Fig. 3), we obtain that for $\beta_z < -(1-2\alpha)\alpha$ the crack is monotonically unstable, whereas for $\beta_z > -(1-2\alpha)\alpha$ the transition from stability to instability occurs in the oscillatory region, i.e., when the dominant zero has an imaginary part. Thus these transition points are given by $z_0 = 1 \pm i\gamma$. To determine the associated (β_x, β_z) at this transition point we separate the equation

$$0 = p(1 + i\gamma)$$

into real imaginary parts. From the resulting two polynomials in γ we eliminate γ. Using Mathematica (Wolfram

Research) we finally get an implicit equation for these (β_1, β_2) at which the transition from oscillatory stability to oscillatory instability occurs

$$
\begin{aligned}
0 = {} & 1024(-1+\alpha)^6(-1+2\alpha) + 32(-1+\alpha)^3(-1+2\alpha)(20-8\alpha-7\alpha^2-3\alpha^3)\beta_1^2 \\
& + (-1+2\alpha)(112-32\alpha-276\alpha^2+184\alpha^3-17\alpha^4+30\alpha^5)\beta_1^4 \\
& + 6(1-2\alpha)(1-\alpha)(1+\alpha)^2(1+2\alpha)\beta_1^6 \\
& + 64(-1+\alpha)^3\alpha(10-17\alpha+3\alpha^2+6\alpha^3)\beta_1\beta_2 \\
& + 4\alpha(112-246\alpha+114\alpha^2+17\alpha^3+30\alpha^4-18\alpha^5-8\alpha^6)\beta_1^3\beta_2 \\
& + 2\alpha(1-\alpha)^2(-39-45\alpha-3\alpha^2+5\alpha^3)\beta_1^5\beta_2 + 4\alpha(1+\alpha)^4\beta_1^7\beta_2 \\
& - 32(-1+\alpha)^3\alpha^2(11-11\alpha+2\alpha^2)\beta_2^2 \\
& - 2\alpha^2(130-200\alpha+75\alpha^2-40\alpha^3+38\alpha^4)\beta_1^2\beta_2^2 \\
& - 2\alpha^2(1+\alpha)^2(-13+5\alpha)\beta_1^4\beta_2^2 - 4\alpha^3(10-7\alpha-2\alpha^2)\beta_1\beta_2^3 + \alpha^4\beta_2^4. \qquad \text{(B1)}
\end{aligned}
$$

From the roots to this equation, the unique transition points are selected by the requirement that $p(1+i\gamma) = 0$ where γ is a function of (β_1, β_2).

In order to obtain the asymptotic behaviour of the oscillatory stable to oscillatory instable transition line in the stability diagram (Fig. 4), we set $\beta_2 \sim c\beta_1^d$ and determine the constant c and d as the biggest possible exponent such that at least two leading terms in eqn (18) still cancel. Indeed this is achieved by

$$
\beta_2 \sim \left(-\frac{4(1+\alpha)^4}{\alpha^2}\beta_1^2 \right)^{1/2}.
$$

In the range of $\beta_2 > 0$ the two transition points from oscillatory to monotonically regions are obtained from the condition that

$$
0 = p(z_0) \qquad \text{and} \qquad 0 = \frac{\mathrm{d}p(z_0)}{\mathrm{d}z_0}
$$

where z_0 is real in this case. Again using Mathematica to eliminate z_0 from these two equations we get

$$
\begin{aligned}
0 = {} & -3456\alpha^6\beta_1 + \alpha^3(13{,}797 - 27{,}756\alpha + 7524\alpha^2 + 128\alpha^3)\beta_1^3 \\
& + 4(27 - 54\alpha - 45\alpha^2 - 683\alpha^3 - 94\alpha^4 - 59\alpha^5)\beta_1^5 - 16(1+\alpha)^4\beta_1^7 \\
& - 3456\alpha^6\beta_2 + 3\alpha^3(9225 - 14{,}880\alpha + 2636\alpha^2)\beta_1^2\beta_2 \\
& + 4\alpha(225 + 45\alpha - 1509\alpha^2 - 361\alpha^3)\beta_1^4\beta_2 - 128\alpha(1+\alpha)^2\beta_1^6\beta_2 \\
& + 375(45 - 44\alpha)\alpha^3\beta_1\beta_2^2 + 400(5 - 13\alpha)\alpha^2\beta_1^3\beta_2^2 - 256\alpha^2\beta_1^5\beta_2^2 \\
& + 3125\alpha^3\beta_2^3.
\end{aligned}
$$

By the same arguments as above, we finally obtain the given asymptotic equations.